Application of SMES Unit to improve the performance of wind turbine conversion system

A. M. Shiddiq Yunus[1], A. Abu-Siada[2] and M. A. S Masoum[2]

[1]Department of Mechanical Engineering, Energy Conversion Study Program, State Polytechnic of Ujung Pandang, Perintis Kemerdekaan KM.10 Makassar 90245, Indonesia

[2]Department of Electrical and Computer Engineering, Curtin University, Perth, WA, Australia.

ABSTRACT

The amount of wind turbine connected to the power grid has significantly increased during the last decade. This has resulted in essential need to establish grid codes. Previously, wind turbine generators (WTGs) were allowed to be disconnected from the network during any disturbance at the grid side to avoid WTGs from being damaged. However, lately, the transmission system operators (TSOs) require WTGs to be stayed connected to provide support to the grid during fault. This new requirement has been regulated in the new grid codes. In this paper, the super conducting magnetic energy storage (SMES) unit is used to enhance the high voltage ride through (HVRT) capability of DFIG based WTG during voltage swell events at the grid side. Two new grid codes are used to verify the ability of the SMES unit to avoid the WTG from being disconnected from the grid.

Introduction

Voltage Swell is one of the common power quality problems in the power system. Voltage swell is defined as an increase in voltage level in the range of 1.1 pu to 1.8 pu for a duration of 0.5 cycle to 1 minute. Voltage swell is mainly caused by switching off a large load, energizing a capacitor bank and voltage increase in an unfaulted phases during a single line-to-ground fault [1]. In the early stages of using WTG, it was allowable to disconnect the WTG from the grid during the event of grid disturbance to avoid WTGs damage. Due to the significant increase in WTGs and the global trend to establish smart grids, the transmission system operators (TSOs) require the connection of WTGs with the grid to be maintained during certain level of faults to provide support to the grid during fault conditions [2]. The WTG equipped with Doubly Fed Induction Generator (DFIG) in conjunction with voltage swell condition at the grid side is studied in this paper. DFIG is selected because it is the most popular installed WTGs over the world. In year 2002 about 46.8 % of the total installed WTGs worldwide were equipped with DFIG [3]. The typical configuration of DFIG is depicted in Fig. 1. The DFIG stator winding is connected directly to the low voltage side of the transformer while its rotor winding is connected to a bidirectional back to back IGBT voltage source converter.
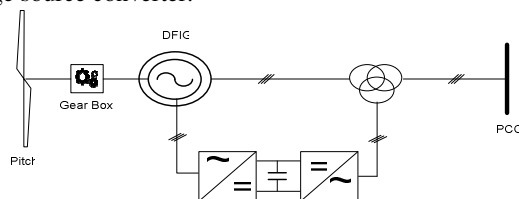

Fig. 1. Typical configuration of WTG equipped with DFIG

Since voltage sag is a common power quality problem in power systems, most of studies are focused on the performance of WTGs during voltage sag [4-10]. Although it is a less power quality problem, voltage swell may also lead to the disconnection of WTGs from the grid. In this paper, The Spain voltage ride through (VRT) and the VRT of US codes shown in Fig. 2 and Fig. 3 respectively [11] are used to comply with the DFIG during voltage swell at the grid side. The voltage ride through of Spain grid code at the point of common coupling (PCC) shows that the maximum voltage ride through is 130% of the nominal voltage for a duration up to 0.5 s in which after the maximum allowable voltage level is limited to 120% for the next 0.5 s. 1 s after the fault occurrence, voltage level must be in the range of 110%-90%. Voltage profile at the PCC has to be in the range of the safety margin shown in Fig. 2 to prevent the disconnection of wind turbine. When the voltage profile is outside the VRT shown in Fig. 2, the wind turbines have to be disconnected from the grid. For high voltage ride through according to US code shown in Fig. 3, voltage must be limited to 120% for maximum duration of 1 s and drops by about 3.3 % every 1s until reaching 4 s from fault occurrence.
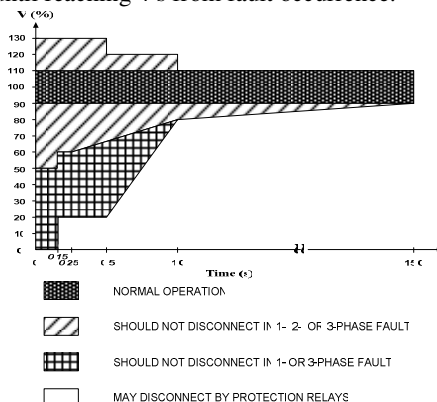

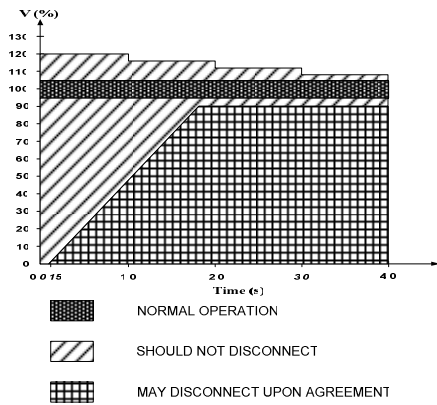
Fig. 2. VRT of Spain grid code

Fig. 3. VRT of US grid code

System under study

The system under study shown in Fig. 2 consists of six-1.5 MW DFIG connected to the AC grid at PCC via Y/Δ step up transformer.
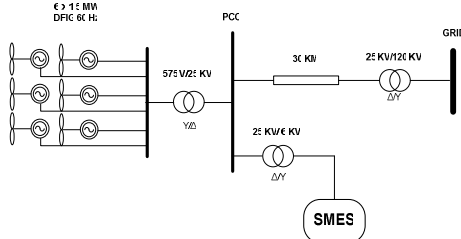

Fig. 4. System under study

The grid is represented by an ideal 3-phase voltage source of constant frequency and is connected to the wind turbines via 30 km transmission line. The reactive power produced by the wind turbine is regulated at 0 Mvar at normal operating conditions. For an average wind speed of 15 m/s which is used in this study, the turbine output power is 1 pu and the generator speed is 1 pu. SMES Unit is connected to the 25 KV bus and is assumed to be fully charged at its maximum capacity of 1 MJ.

SMES Configuration and Control Algorithm

Superconducting coil stores energy within a magnetic field created by the flow of direct current in a coil which should be maintained within superconductivity state through immersion in liquid Helium at 4.2 K in a vacuum - insulated cryostat. A power electronic converter interfaces the SMES and the grid to control the energy exchange between them. With the rapid development of materials that exhibit superconductivity closer to room temperatures, this technology will become economically viable in the next few years [12]. The overall efficiency of SMES depends on the coil material and the configuration used and it is in a typical range of 90-95% [13-15]. The high efficiency of the SMES unit is achieved by its lower power loss because electric currents in the coil encounter almost no resistance and there are no moving parts included. The configuration of SMES unit used in this paper is shown in Fig. 5. Hysteresis current regulator along with fuzzy logic control are employed to control the active and reactive power exchange between the SMES unit and the grid as will be explained in the following sub sections.
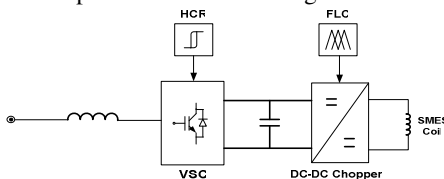

Fig. 5. SMES configuration

Hysteresis Current Regulator (HCR)

To control the direction of power flow from the voltage source converter (VSC), hysteresis current regulator (HCR) is preferred based on its advantages, which include ease implementation, fast dynamic response, maximum current limit and its insensitivity to load parameter variations [16]. The solid state switching component of VSC consists of six-IGBT to support the optimal application of SMES unit since it simplifies the converter design and enables considerably higher switching frequency compared to bipolar junction transistor [17]. As shown in Fig. 6, HCR is comparing the 3-phase line currents with the reference current which is dictated by the I_D* and I_Q* references. The value of I_D* and I_Q* are generated through conventional PI controllers from the error values of VDC and VS. The capacitor is used to store a constant DC voltage that is maintained by VSC controller as shown in Fig. 6. The fixed band of Hysteresis Current Regulator, however, can cause interference between phases (referred as inter-phases dependency) which can lead to high switching frequency. To maintain the advantages of the hysteresis methods, this phase dependency can be minimized by using phase-locked loop (PLL) technique to maintain the converter switching at a fixed predetermined frequency [18].
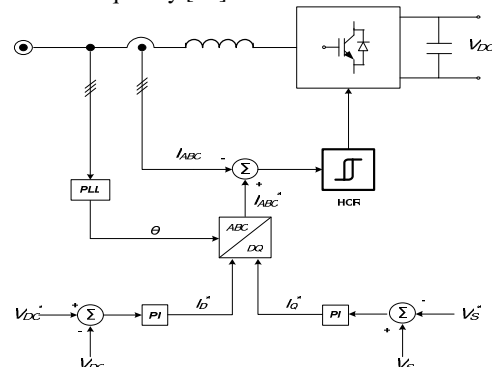

Fig. 6. Control algorithm of the SMES

Fuzzy Logic Controller

The SMES coil is connected to the VSC by a DC link. The charging and discharging process of SMES energy is determined by fuzzy logic control (FLC) of class D two-quadrant DC-DC chopper as shown in Fig. 7. The active power from the generator (PG) and the current in the superconducting coil (ISM) are used as inputs to the fuzzy logic controller.
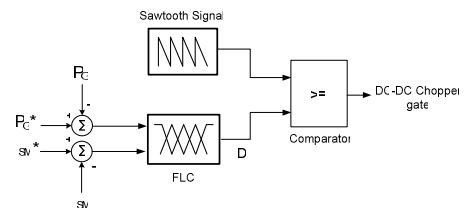

**Fig. 7. Control algorithm of DC-DC Chopper**

The output of the FLC is the duty cycle (D) which is compared with 1000 Hz saw-tooth signal to produce DC-DC chopper signal which determines the charging/discharging process of SMES energy. The operation range of the duty cycle is given in Table I.

If the duty cycle (D) is equal to 0.5, no action will be taken by the coil and system is defined as normal, when the grid power is reduced, D, will be reduced accordingly in the range of 0 to 0.5 and the stored energy in the SMES coil will be transferred to the grid. Charging process of the coil takes place when D is in

the range of 0.5 to 1. The model is built using the graphical user interface tool provided by MATLAB. Each input was fuzzified into five sets of gaussmf type of membership function (MF). The Gaussian curve is a function of a vector, x, and depends on parameters σ and c as given by:

$$f(x;\sigma,c) = e^{\dfrac{-(x-c)^2}{2\sigma^2}} \qquad (1)$$

Where σ is a variable that determines the position of the centre of the peak and c is a variable that determines the width of the bell curve. The corresponding membership functions for each input variable are shown in Fig. 8 and Fig. 9.
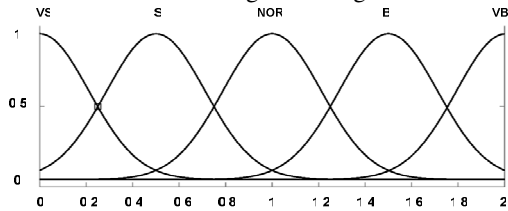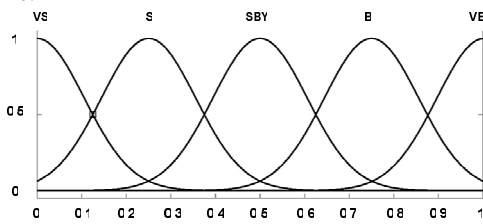
VS=Very Small, S=Small, NOR=Normal, B=Big, VB=Very Big

Fig. 8 Input variable MF – Pg (pu)
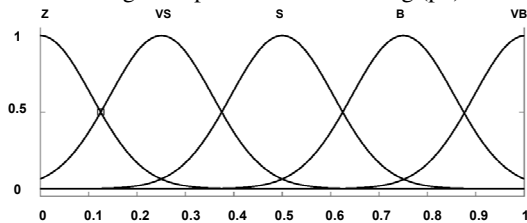
Z=Zero, VS=Very Small, S=Small, B=Big, VB=Very Big

Fig. 9. Input Variable MF – ISM (pu)

Result of fuzzification from each input was then applied with fuzzy operator in the antecedent and related consequence, by application method. The membership functions for the output variable (duty cycle) are considered on the scale 0 to 1 as shown in Fig. 10.

VS=Very Small, S=Small, SBY=Stand-By, B=Big, VB=Very Big

Fig. 10. Output variable MF – Duty cycle

Centre-of-gravity which is widely used in fuzzy models was used for defuzzification process where the desired output z_0 is calculated as [19]:

$$z_0 = \frac{\int z.\mu_c(z)dz}{\int \mu_c(z)dz} \qquad (2)$$

where $\mu_c(z)$ is the membership function of the output.

The variation range in SMES current and DFIG output power and the corresponding duty cycle are used to develop a set of fuzzy logic rules in the form of (IF-AND-THEN) statements to relate the input variables to the output. The duty cycle for any set of input data (P_G and I_{SM}) can be evaluated from the surface graph shown in Fig. 11.
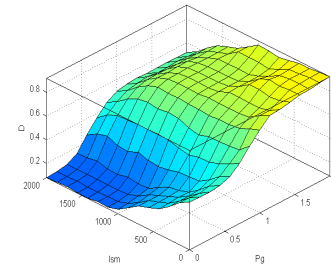

Fig. 11. Surface graph-Duty cycle

Simulation result

Voltage swell of 1.4 pu is applied at the grid side and is assumed to start at 2 s and cleared out at 2.13 s. As can be seen from Fig. 12 and the zoomed area shown in Fig. 13, without SMES, voltage at the PCC bus will increase to 1.35 pu. By applying the HVRT of Spain grid code, the WTGs equipped with DFIG have to be disconnected from the grid in this case. The same action will be taken by TSOs to disconnect the WTGs if HVRT of US grid code is applied to this system. However, when SMES unit is connected to the PCC, the high voltage level at the PCC will be reduced below the maximum voltage level of HVRT of both Spain and US grid codes. Therefore, disconnection can be avoided by connecting SMES to the PCC bus. When the fault is cleared at 2.13 s, the voltage at the PCC will be reduced to 0.82 pu when the SMES unit is not connected to the system while with the SMES unit, this level is increased to 0.9 pu as can be seen in Fig. 2.
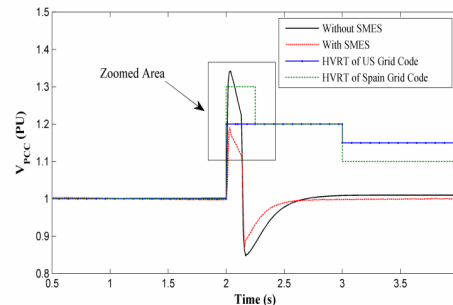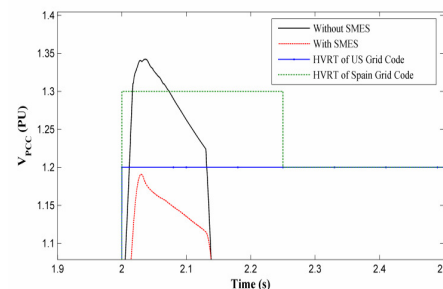

Fig. 12. Voltage response at the PCC

Fig. 13. Zoomed area of voltage response at the PCC

The behavior of DFIG during voltage swell at the grid side can be analyzed from Fig. 14 and Fig. 15. During voltage swell, the active power produced by the generator will suddenly increase to 1.38 pu and will be reduced when fault is cleared similar to the voltage at the PCC. With SMES connected to the system overshooting of power can be reduced as shown in Fig. 14. Without the SMES unit, the reactive power produced by DFIG transferred to the grid during voltage swell is 0.8 pu. However, by connecting the SMES unit, DFIG only needs to supply 0.3 pu during the event of voltage swell as shown in Fig. 15.
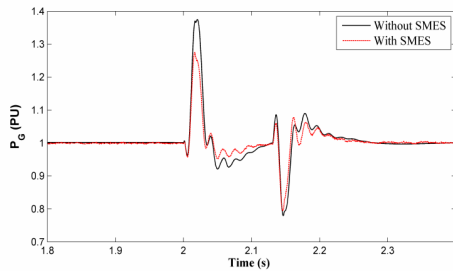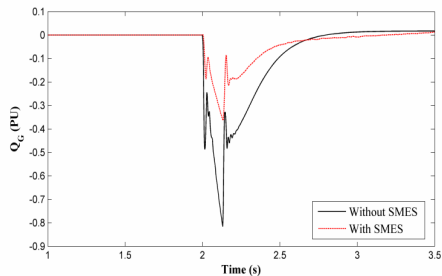
Fig. 14. Active power output of DFIG
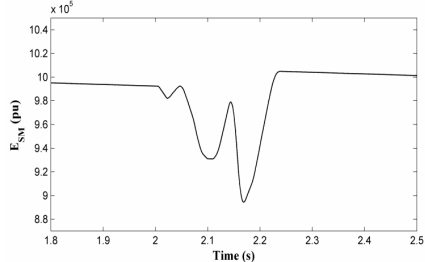

Fig. 15. Reactive power output of DFIG

Fig. 16. Energy behavior of SMES coil
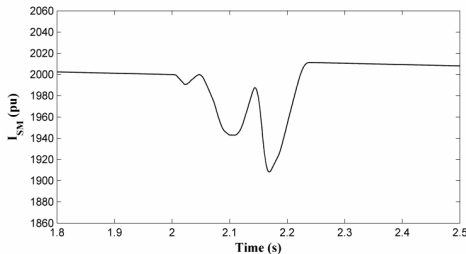

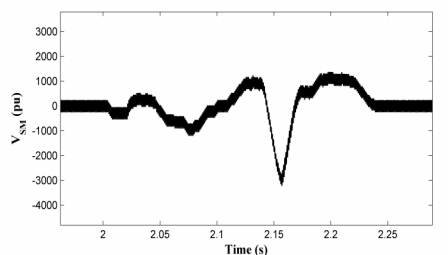**Fig. 17. Current behavior across the SMES coil**

Fig. 18. Voltage profile of SMES coil

The behavior of the SMES coil during the fault can be investigated through Fig 16 to Fig.18 which respectively show the SMES coil stored energy, SMES current and the voltage across the coil. The SMES coil energy is 1 MJ during normal operating conditions, when voltage swell occurs, SMES coil instantly discharges its energy into the grid as shown in Fig. 16. The characteristic of SMES current shown in Fig. 17 is similar to the energy stored in the coil. The charging and discharging process of SMES coil can also be examined from the voltage across SMES coil (V_{SM}) shown in Fig. 18. During normal operating conditions, V_{SM} is equal to zero, it goes to negative value during discharging process and will return back to zero level after the fault is cleared.

Conclusion

This paper investigates the use of SMES unit to enhance the HVRT of wind energy conversion system to comply with the grid codes of Spain and US grid codes. Results show that, without the use of SMES unit, WTGs must be disconnected from to avoid the turbines from being damaged. However, the proposed controller of the SMEs unit can significantly improve the HVRT capability of the WTGs and their connection to the grid can be maintained.

Acknowledgement

Reference

[1] E. F. Fuchs and M. A. S. Masoum, "Power Quality in Power Systems and Electrical Machines," Elsevier, 2008.

[2] J. G. Slootweg, S. W. H. de Haan, H. Polinder, and W. L. Kling, "General model for representing variable speed wind turbines in power system dynamics simulations", *Power Systems, IEEE Transactions on,* vol. 18, pp. 144-151.2003

[3] T. Ackermann, Wind Power in Power System*,* West Sussex: John Wiley and Sons Ltd, pp. 65.2005

[4] R. K. Behera and G. Wenzhong, "Low voltage ride-through and performance improvement of a grid connected DFIG system," in *Power Systems, 2009. ICPS '09. International Conference on*, pp. 1-6.2009

[5] S. Hu and H. Xu, "Experimental Research on LVRT Capability of DFIG WECS during Grid Voltage Sags," in *Power and Energy Engineering Conference (APPEEC), 2010 Asia-Pacific*, pp. 1-4,

[6] K. Lima, A. Luna, E. H. Watanabe, and P. Rodriguez, "Control strategy for the rotor side converter of a DFIG-WT under balanced voltage sag," in *Power Electronics Conference, 2009. COBEP '09. Brazilian*, pp. 842-847.2009

[7] L. Trilla, O. Gomis-Bellmunt, A. Junyent-Ferre, M. Mata, J. Sanchez, and A. Sudria-Andreu, "Modeling and validation of DFIG 3 MW wind turbine using field test data of balanced and unbalanced voltage sags", *Sustainable Energy, IEEE Transactions on,* vol. PP, pp. 1-1.2011

[8] Y. Xiangwu, G. Venkataramanan, P. S. Flannery, and W. Yang, "Evaluation the effect of voltage sags due to grid balance and unbalance faults on DFIG wind turbines," in *Sustainable Power Generation and Supply, 2009. SUPERGEN '09. International Conference on*, pp. 1-10.2009

[9] Y. Xiangwu, G. Venkataramanan, P. S. Flannery, W. Yang, D. Qing, and Z. Bo, "Voltage-Sag Tolerance of DFIG Wind Turbine With a Series Grid Side Passive-Impedance Network", *Energy Conversion, IEEE Transactions on,* vol. 25, pp. 1048-1056

[10] W. Yulong, L. Jianlin, H. Shuju, and X. Honghua, "Analysis on DFIG Wind Power System Low-Voltage Ridethrough," in *Artificial Intelligence, 2009. JCAI '09. International Joint Conference on*, pp. 676-679.2009

[11] Alt, x, M. n, Go, O. ksu, R. Teodorescu, P. Rodriguez, B. B. Jensen, and L. Helle, "Overview of recent grid codes for wind power integration," in *Optimization of Electrical and Electronic Equipment (OPTIM), 2010 12th International Conference on*, pp. 1152-1160, 2010

4319

Shiddiq Yunus et al./ Elixir Elec. Engg. 38 (2011) 4315-4319

[12] L. Freris and D. Infield, Renewable Energy in Power System, Wiltshire: A John Wiley & Sons, pp. 143-144.2008

[13] P. F. Ribeiro, B. K. Johnson, M. L. Crow, A. Arsoy, and Y. Liu, "Energy storage systems for advanced power applications", *Proceedings of the IEEE*, vol. 89, pp. 1744-1756.2001

[14] S. C. Smith, P. K. Sen, and B. Kroposki, "Advancement of energy storage devices and applications in electrical power system," in *Power and Energy Society General Meeting - Conversion and Delivery of Electrical Energy in the 21st Century, 2008 IEEE*, pp. 1-8.2008

[15] H. Chen, T. N. Cong, W. Yang, C. Tan, Y. Li, and Y. Ding, "Progress in electrical energy storage system: A critical review", *Progress in Natural Science*, vol. 19, pp. 291-312.2009

[16] K. Bong-Hwan, K. Tae-Woo, and Y. Jang-Hyoun, "A novel SVM-based hysteresis current controller", *Power Electronics, IEEE Transactions on*, vol. 13, pp. 297-307.1998

[17] A. Carlsson, The Back to Back Converter, Lund: Department of Industrial Electrical Engineering and Automation Lund Institute of Technology, pp. 7.1998

[18] L. Malesani and P. Tenti, "A novel hysteresis control method for current-controlled voltage-source PWM inverters with constant modulation frequency", *Industry Applications, IEEE Transactions on*, vol. 26, pp. 88-92.1990

[19] H. Li and M. M. Gupta, Fuzzy Logic and Inteligent System, Massachusetts: Kluwer Academic Publisher, pp. 8. 1995

Table 1 Rules and Cycle

Duty Cycle (D)	SMES Coil Action
D = 0.5	standby condition
$0 \leq D < 0.5$	discharging condition
$0.5 < D \leq 1$	charging condition